CONSTRAINTS ON THE DYNAMICAL STABILITY OF A PLANET IN THE HABITABLE ZONE OF THE STAR GLIESE 581. Zs. Tóth[1] and I. Nagy[2], [1]Department of Geosciences, University of Bremen, Klagenfurter Strasse, 28359 Bremen, Germany, email: zsuzsanna.toth@gmail.com, [2]Department of Natural Science, National University of Public Service, Hungária körút 9-11, 1101 Budapest, Hungary, i.nagy@astro.elte.hu.

Introduction: Gliese 581 is a M3V red dwarf star approx. 22 light years away. Radial velocity (RV) measurements suggest that it has a planetary system of four planets (b-e) [1- 3], with the possibility of two additional, unconfirmed planets g and f [4-10]. Gliese 581 e is a low mass planet with a minimum mass of 1.9 Earths and orbital period of 3.15 days; Gliese 581 b is a Neptune-mass planet on a 5.36-day orbit; planet c and d are two super-Earth sized planets with orbital periods of 12.9 and 67 days. The orbital and physical parameters of the planets are summarized in Table 1. Recently, a cold debris disk was also discovered around the star with an inclination between $30^o < i < 70^o$ to the line of sight. Assuming the disk plane and the planetary orbits are co-planar, this makes the planetary masses no more than ~1.6 times their measured minimum masses [11].

Table 1: Astrocentric, circular, 4-planet model of the Gliese 581 exoplanetary system [4].

Planet	*P* (days)	M_{min} (M_{Earth})	*a* (AU)	*e*	*l* (deg)
e	3.15	1.84	0.028	0	138.5
b	5.37	15.98	0.04	0	338.9
c	12.93	5.4	0.073	0	175.2
d	66.71	5.25	0.22	0	235.8

The conservative habitable zone (HZ) around Gliese 581 is in the region between planet c and d – these super-Earths are near to, but outside the HZ [12]. Gliese 581 g, if exists, is a 2 M_{Earth} planet in the middle of the star's HZ [4]. Planet g would likely be a rocky planet, and favorable atmospheric conditions may permit the presence of liquid water on its surface. A planet in the habitable zone is likely to be tidally locked, because the extremely close distances to the star cause tidal locking within short timescales [12-14]. However, the side of the planet facing the star might have extensive cloud cover increasing its Bond albedo and reducing the temperature differences between the two sides significantly [15].

Several new analyses of the RV data questioned the existence of planet g. With the addition of new RV measurements, however, its periodic signal could become statistically significant. Its orbital parameters as well as its mass could be modified, so we investigate generally the possibility of a fifth low-mass planet in the HZ of Gliese 581 from a dynamical point of view.

Methods: Numerical integrations of the planetary orbits were performed using the method of Lie-integration with an adaptive step-size. To characterize stability, stability maps were created as a function of the semi-major axis and eccentricity. On the maps, chaotic motion is identified by the Lyapunov characteristic indicator (LCI) and the relative Lyapunov indicator (RLI), while dynamical stability is described with the maximum eccentricity that the planets have reached over the time of the integrations. The model parameters were taken from the 4-planet RV fit of [4], which includes planet b, c, d and e on initially zero eccentricity orbits. For the mass of Gliese 581 we took 0.31 M_{Sun}. We made the assumption of coplanarity of all orbits. The test planets initial parameters were varied: the semi-major axis with steps of Δa = 0.001 AU, and the eccentricity with steps of Δe = 0.01. e_{max}, the LCI and the RLI were calculated for the test planet and are plotted for the grid of different *a*, *e* in the figures.

Results: The 4-planet model with an additional massless test planet was integrated for 5000 P_{test} for i = 30, 50, 70º, where P_{test} is the orbital period of the test planet, in order to find regions of possible orbital stability in the HZ. Since from the RV data only the quantity *Msini* is determined, mass of the exoplanets are constrained only by a lower limit. With decreasing *i*, thus with increasing *M*, the system could become unstable due to dynamical interactions.

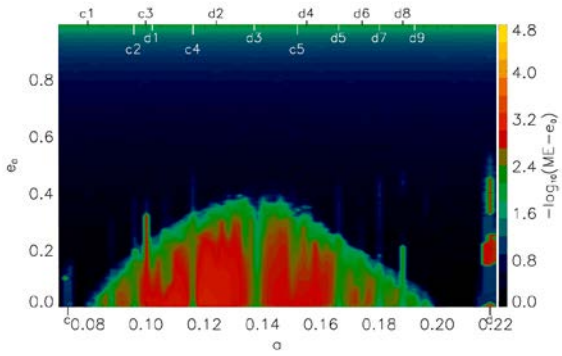

Fig. 1: Average maximum eccentricity of a fifth massless test planet for 8 starting positions. Stable: towards yellow, unstable: towards black.

In all cases though, the variations of the semi-major axis and eccentricities of the planets are not significant

by the end of the integration, so the system has this basic stability for the inclination range of the debris disk and thus higher planetary masses. The average e_{max} that the test planet reached over the integration time for 8 different starting positions (Δl = 45º between l = 0-315º) is plotted in Fig.1. An extensive stable region exists within the HZ for a fifth planet. Several mean-motion resonances (MMRs) between the test planet and planet c or d were identified in the HZ (on top of Fig.1.; see also in [8]), however, none of these resonances overlap, which could cause instability in the planetary system.

In another integration, also for 5000 P_{test}, the semi-major axis of the test planet was varied in the region of the HZ as a function of the eccentricity of planet d until its orbit would cross the orbit of planet c. As Fig.2 shows, the more elliptic planet d's orbit is, the further away planet g has to be from it in order to remain stable. The stability of a planet in the HZ is strongly dependent on the eccentricity of the adjacent planet d.

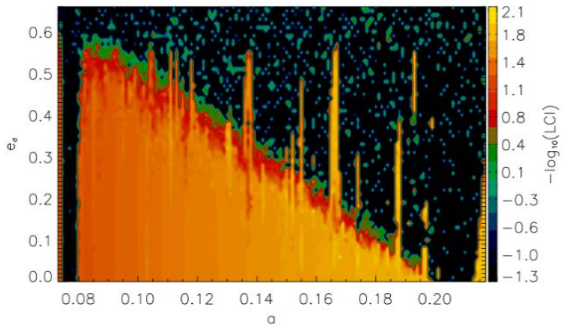

Fig. 2: LCI of the test planet. Stable: towards yellow, unstable: towards black.

We also checked for which range of eccentricity the test planet would remain stable in the HZ. The integration ran for 5000 P_{test} and for 8 different starting positions again. This time the chaos indicator RLI of the test planet was calculated and the average of the 8 values is plotted on the *a*-*e* stability map in Fig.3. The RLI reveals that the dynamical stability of planet in the HZ greatly depends on the eccentricity, and this planet would only be stable on circular or nearly circular orbits in this region. Even this small stable region (yellow and red colors) close to zero eccentricity is not entirely continuous, probably as a consequence of the above mentioned MMRs identified between the fifth planet and planet c and d.

Finally, we integrated the orbit of the test planet between planet c and d within the HZ for 5000 P_{test}, by randomly choosing its 6 orbital elements using the Monte Carlo method. Out of 192035 configurations, 9.1% (17535) of the orbits are dynamically stable. With increasing inclination, thus decreasing planetary masses, the number of stable orbital configurations increase: from 7% (i = 0 to 5º) to 11% (i = 85 to 90º). In the closer vicinity of the unconfirmed low-mass planet g, between 0.11-015 AU, out of 89462 orbital configurations 6.4% are stable. Increasing inclination increases the number of stable orbital configurations here too: from 4.1% (i = 0 to 5º) to 8.2% (i = 85 to 90º).

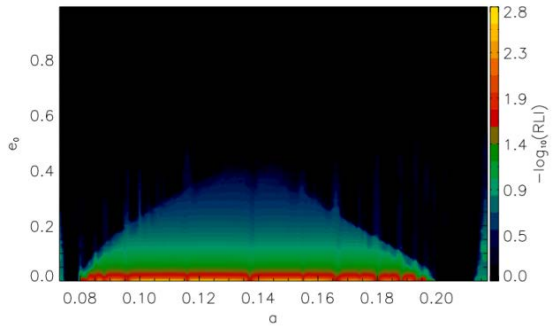

Fig. 3: Average RLI of the test planet for 8 different starting positions. Stable: towards yellow, unstable: towards black.

Conclusions: There is an extensive, dynamically stable region in the HZ of Gliese 581 for a fifth planet. A planet in the HZ would also remain stable for the inclination range 30º < i < 70º assuming coplanarity, that is for higher planetary masses than the minimum mass. Though, the eccentricity of a planet in the HZ would be coupled to the eccentricity of the outer planet d. Moreover, this planet would be only stable on circular or very low-eccentricity orbits.

References: [1] Bonfils. X. et al. (2005) *A&A, 443*, 15-18. [2] Udry, S. et al. (2007) *A&A, 469*, 43-47. [3] Mayor, M. et al. (2009) *A&A, 507*, 487-494. [4] Vogt, S. S. et al. (2010) *ApJ, 723*, 954-965. [5] Gregory, P. C. (2011) *MNRAS, 415*, 2523-2545. [6] Tuomi, M. (2011) *A&A, 528*, L5. [7] Vogt, S. S. et al. (2012) *AN, 333*, 561-575. [8] Tadeu dos Santos, M. et al. (2012) *CeMDA, 113*, 49-62. [9] Makarov, V.V. et al. (2012) *ApJ, 761*, 83. [10] Tuomi, M. and Jenkins, J. S. (2012) *A&A, submitted.* [10] Hatzes, A.P. (2013) *AN, 334*, 616-624. [11] Lestrade, J.-F. et al. (2012) *A&A, 548*, A86. [12] Selsis, F. (2007) *A&A, 476*, 1373-1387. [13] Barnes, R. et al. (2008) *Astrobiology, 8 (3)*, 557-568. [14] Barnes, R. et al. (2009) *ApJ, 700*, L30-L33. [15] Yang, J. et al. (2013) *arXiv:1307.0515* [astro-ph.EP].